Co-published by
Institute of Fluid-Flow Machinery
Polish Academy of Sciences
Committee on Thermodynamics and Combustion
Polish Academy of Sciences

http://www.imp.gda.pl/archives-of-thermodynamics/

Comparative experimental analysis of fluid flow in a concentric tube exchanger having semi hollow cylindrical macro inserts with nanofluid and base fluid

Shivasheesh Kaushik[a*], Vikas Singh Mahar[b], Satyendra Singh[c], Rahul Kshetri[d], Bhupendra Kumar[d], Jagdish Singh Mehta[e], Ashwarya Raj Paul[f], Satish Kumar[f], Samriddhi Vashisth[f], Raj Singh Pundir[f], Amit Kumar[g]

[a*]Assistant Professor, Department of Mechanical Engineering, S. C. E. Dehradun, India.
[b]Assistant Professor, Department of Electrical and Electronics Engineering, S. C. E. Dehradun, India.
[c]Professor, Department of Mechanical Engineering, B.T.K.I.T. Dwarahat, India.
[d]Assistant Professor, Department of Mechanical Engineering, Dr. A.P.J.A.K.I.T. Tanakpur, India.
[e]Assistant Professor, Department of Mechanical Engineering, Graphic Era Hill University, Bhimtal, India.
[f]Scholar, Department of Mechanical Engineering, S. C. E. Dehradun, India.
[g]Assistant Professor, Department of Mechanical Engineering, G.B.P.I.E.T., Pauri, India.
*Corresponding author email: skaushik@sce.org.in

Received: 06.07.2023; revised: 25.10.2023; accepted: 14.01.2024

Abstract

Nanofluids represent a novel category of advanced heat transfer fluids composed of nanoparticles within a size range of 1-20 nm dispersed in a base fluid such as water. Contemporary research predominantly focuses on incorporating nanoparticles like Al_2O_3 and ZnO into the water at a 0.1% volume fraction to create nanofluids. Recent investigations aim to optimize thermal performance by introducing nanoparticles into the base fluids and inducing turbulence through various macro-inserts. Key factors influencing heat exchanger efficiency enhancement include geometric parameters, thermal conductivity and volume fraction. This study endeavours to analyse the thermal and fluid flow characteristics of a proposed nanofluid, augmenting thermal transfer through computational simulations and experimental validation, achieving an error margin of 3%-5%. The impact of rectangular micro inserts, with dimensions of 4 cm in height and longitudinal spacings of 5 cm and 11.5 cm, on the heat transfer rate is examined to enhance fluid flow turbulence. Results indicate that among different geometric profiles, the insert with a spacing of 11.5 cm demonstrates superior performance, yielding higher heat transfer rates and Nusselt numbers. This research holds significant implications for various industries including thermal, power, aviation, space and automotive sectors, particularly in the utilization of concentric tube heat exchangers across diverse applications. By exploring novel geometrical and fluid domains within heat exchangers, this study unveils promising avenues for enhancing the heat transfer efficiency compared to conventional methods, highlighting the potential for further investigation into alternative materials and configurations for heat elimination enhancement.

Keywords: Longitudinal spacing; Macro insert; Fin height; Nanofluid; Orientation; Ultrasonication

Vol. 45(2024), No. 2, 205–212; doi: 10.24425/ather.2024.150866

Cite this manuscript as: Kaushik, S., Mahar, V.S., Singh, S., Kshetri, R., Kumar, B., Mehta, J.S., Paul, A.R., Kumar, S., Vashisth, S., Pundir, R.S., & Kumar, A. (2024). Comparative experimental analysis of fluid flow in concentric tube exchanger having semi hollow cylindrical macro inserts with nanofluid and base fluid. *Archives of Thermodynamics*, 45(2), 205–212.

1. Introduction

Nanofluids have admirable physio-chemical, thermal and heat transfer properties [1, 2]. Thermal performance and pressure drop in heat exchangers are examined by many researchers but specifically good thermal performance is achieved for TiO_2–H_2O nanofluids with deionised H_2O as a base fluid. For the nanoparticle concentration of w = 0.1%, 0.3% and 0.5%, the

Nomenclature

A – area of pipe, m^2
C – capacity rate, J/K
C_p – specific heat of fluid, J/(kg K)
D – diameter of pipe, m
h – heat transfer coefficient, W/(m^2 K)
H – heat transfer coefficient, W/(m^2 K)
K – thermal conductivity of fluid, W/(m K)
L – length of pipe, m
m – mass flow rate of fluid, kg/s
ΔP – differential pressure, bar
Q – heat transfer rate of fluid (*htr*), J/s
Q_{ds} – fluid discharge, lps
T – temperature, K
u – fluid velocity, m/s
U – overall heat transfer coefficient, W/(m^2 K)
V – fluid volume, m^3

Greek symbols

η – efficiency
μ – dynamic viscosity, Pa s
ρ – density, kg/m^3

Subscripts and Superscripts

cf – cold fluid
ds – discharge
f – fluid
hf – hot fluid
i, in – inner
o, out – outer
st – smooth tube
s – simulation
thpf – thermal performance factor

Abbreviations and Acronyms

CSTHE – concentric spiral tube heat exchanger
CTAB – cetyl trimethyl ammonium bromide
CTHE – concentric tube heat exchanger
GI – galvanized iron
HCHE – helical coil heat exchanger
HTC – heat transfer coefficient
LMTD – logarithmic mean temperature difference
LS – longitudinal spacing
NTU – number of transfer units
TE – tube exchanger
TPCR – tapered perforated conical ring
TPF – thermal performance factor

heat transfer rate increases by 10.8%, 13.4% and 14.8%, respectively, as compared to H_2O. On the tube side, the pressure drop increases by 51.9%, and on the shell side by 40.7% (both sides operate with nanofluids and are corrugated). Also, the number of transfer units (NTU) and effectiveness is increased [1]. Physical properties of nanofluids have been evaluated previously in the literature, these properties have two parameters (optical and geometrical). In both cases, the working fluid is H_2O; the viscosity and thermal conductivity depend on the temperature. The results predict an improvement in the Nusselt (Nu) number at the shell side by 10%, at the coil side by 0.8%. The heat transfer coefficient decreased when Nu of both sides was increased, Nu of the coil side more than twice that of the shell side Nu number. (temperature of coil 81.49–82.74°C, temperature of shell 66.65–60.95°C, Reynolds (Re) number of coil 1000–27 000, Re of shell 2000–49 000) [3], where the heat transfer performance has been analyzed for a screw pitch and nano particle mass fraction with a spiral tube. The results predicted that the Nu number increases when the screw pitch decreases and the nanoparticle mass fraction increases. The screw pitch of S = 10 cm achieved the smallest heat transfer rate but it can be improved by 49.8–62.0% with the spiral tube rotation angle β = 45° and β = 90° [4]. Experimental investigations have been performed on the heat transfer and pressure drop for Al_2O_3-H_2O nanofluids with small volume fractions such as 0.1%. The Nusselt number increased by 12.24 compared to that of distilled H_2O. While comparing the pressure drop with that of distilled H_2O, then the increasing trend was shown by the pressure drop. For the test set-up made of stainless steel and 2 wire coil inserts with a pitch ratio 2 and 3, the Nusselt number increased by 15.91 and 21.53 as compared to that of distilled H_2O. For Al_2O_3 nano particles of size 43 mm, the optimum Nu number value was 2275 [5].

Some studies focused on the effect of nano particle size on the heat transfer and pressure drop properties for the laminar forced convection in a micro channel subject to a constant heat flux. Here, aqueous nanofluids containing dispersions of Al_2O_3 and TiO_2 have been simulated using a discrete phase model (DPM) for a range of particle size between 20–200 nm. The change in hydrothermal properties of nanofluids with the diameter was better observed at a higher particle concentration. The maximum differences in the heat transfer rates and friction factors of 11% and 20% were observed within the range of particle size 20–200 nm for the particle concentration of 2% [6]. In previous studies, a two step method has been adopted to prepare $NaNO_3$–Al_2O_3 nanofluid, where the neutron activation analysis (NAA) and the modulated differential scanning calorimeter (MDSC) have been used to measure the specific heat. Results predicted that for Al_2O_3 nanoparticles dispersed in $NaNO_3$ with a 60-mole fraction or for Al_2O_3 nanoparticles dispersed in KNO_3 with a 40-mole fraction, the actual value of specific heat changes less than by 2%. The mass fraction of Al_2O_3 was 0.78%. The results conclude that an enhancement of 30.6% in mass fraction of Al_2O_3 nano particles yields an increase in specific heat value of less than 4%. During fabrication, Al_2O_3 nanoparticles lost 20% to 40% of their nominal content and their fraction expanded nominally by up to 41% [7].

The proposed paper analyses the behaviour of convective heat transfer and thermal conductivity of nanofluids (CuO–water, CuO–ethylene glycol (EG)) and (TiO_2–water, CuO–EG) in laminar and turbulent flow and it was clearly reported that the thermal conductivity rises with the concentration of nano particles and a rise in temperature. The main purpose of using nano-

fluids rather than the base fluid is the enhancement of the heat transfer rate [8]. Numerical and experimental investigations have been done to perform the heat transfer analysis of various heat exchangers, like a solar air heater based on the absorber plate [9–11], perforation based tapered hollow conical rings (THCR) [12], shell-tube type heat exchangers based on a helical coil [13–15], with diverse fluids like air, water and nanofluid [12–15], or to analyse the location of fins in LED [16]. Some researchers presented diverse properties of sensible materials [17–18], some worked on diverse sensible materials such as rock, dry clay, nylon and teflon for analysing thermal behaviour in a packed bed (PB) and used air as a medium [19–21], whereas some used flue gas as a medium for thermal storage in a packed bed [22]. Some specific properties are important for further utilization of nanofluids in various applications. A wide range of heat exchangers are used in various engineering applications for heat transfer between two or more fluids for both cooling and heating processes. Some researchers focus their attention on the pipe bend loss effects, for improvement of performance of the concentric tube heat exchanger (CTHE), and some analyse the impact of flow velocity through pipes in a conventional and protruded cyclone separator for segregation of ash from hot air [23,24].

Increasing the concentration of nano particles in the base fluid improves the heat transfer rate as reported in some literature [8,14]. Many researchers work on the performance, keeping an eye on environmental aspects [13–15], while analysing flow and heat transfer parameters of nanofluids in spiral tubes with diverse fluids like water [12–15], diverse bio-oils or bio-fuels and nanofluids [15,25] for power plant applications.

Recently, micro channels attract the researchers' attention because of their tremendous performance in a compact size for a wide range of heat transfer applications, especially for machine automation and mobile equipment. The main objective of micro-channel technology is to increase product longevity with minimum maintenance [26,27]. A recent trend in this scope is to analyse the effects of geometrical domain of the micro channels [28–29], or mini channels [30,31], and the fluid domain like nanofluid, specifically for enhanced thermal behaviour of CTHE [28–31].

The present work is based on diverse gaps in the past literature. A brief analysis of research trends in diverse exchangers, design, materials and fluids is shown in Table 1. The methodology of the present work is based on solving steady state problems of forced convection through CFD, FEM, etc. [32]. The novelty of the present work is to enhance the efficiency and performance of a flat plate collector by two diverse approaches, that is, first the installation of a new geometrical design of the heat pipe having a semi hollow cylindrical macro insert inside the copper tube of the flat plate collector, and second is the flow of a modified hybrid nanofluid.

Table 1. Research trend of tube exchanger (TE).

Author	Set-up details
Qi et.al. (2019) [2]	Researchers used only normal double-tube HE for analyzing the effect of thermal transfer with nanofluid.
Chamsa-ard et.al. (2017) [1]	Corrugated TE has been used to evaluate the impact of nanofluid on thermal behaviour.
Zhai et.al. (2019) [4]	Researchers used spiral TE with diverse geometrical parameters like pitch and orientation angle for analyzing the effect of geometry with nanofluid on thermal characteristic.
Chandrasekar et.al. (2010) [5]	Coil insert has been used to enhance the performance of CTHE and pipe exchanger with nanofluid.
Ambreen et.al. (2018) [6]	Researchers analyzed the effect of nanofluid particle size on thermo-hydraulic performance of micro channel.
Kumar et.al. (2018) [8]	Researchers used bundle TE for analyzing the effect of different nanofluid particle sizes with diverse base fluids on thermal and flow parameters.
Uniyal et.al. (2021) [12]	Auhtors used TPCR TE for enhancement of performance of circular air duct.
Kaushik et.al. (2020) [13]	Authors analyzed the flow and thermal attributes of diverse hybrid nanofluid in a spiral coil for enhancement of performance in CTHE.
Kanojia et.al. (2021) [20]	Packed bed was filled with sensible material pebbles, storing heat energy for space heating.
Shrivastav et.al. (2022) [11]	Wedge shape exchanger was used as an absorber to enhance the performance of air heaters.

2. Materials and methods

The selection of nanofluid material for the proposed research work was completely based on the literature survey [14,15]. Going through multiple research papers, the first point of consideration was what nano particles are being popularly used and why they are so popular. The most popular nano particles in terms of cost and properties were identified as Al_2O_3, ZnO and CuO, as compared to other nano particles, all shown in Table 2.

It could be noted that the CuO nanofluid shows a linear behaviour in its conductivity. While changing the size and concentration of Al_2O_3, the thermal conductivity changes non-linearly [33]. Al_2O_3 and ZnO show more diversity in their properties. The preparation of an Al_2O_3 + ZnO + H_2O nanofluid sample is based on the technique of ultrasonication, where Al_2O_3 and ZnO are mixed in water at a 0.005% volume fraction each with 0.51 ml of CTAB surfactant [14,15] through the mechanical string process. After that, a mechanical string sample is transferred to the ultrasonication tub for 6 hours of ultrasonication. The finally prepared sample is ready for the evaluation of its physio-chemical properties experimentally, through the use of a hydrometer for density measurements, and a calorimeter for thermal conductivity and specific heat measurements as shown in Table 2. The experimental values were further validated with the help of a numerical model [14,15].

In this study, the experiment on a heat pipe with macro inserts is performed in a test set-up as shown in Fig. 1. This picture presents the schematic description of the running procedure of

set-up used during experimental work. the accuracy of the measurements is attained at the level of ±0.5%. The computational analysis is carried out using the ANSYS software. Heat pipes with different spacing and orientation of semi hollow cylindrical macro inserts were used in this study. The spacing was 5.5 cm, or alternatively 11.5 cm, whereas the height of macro inserts was 4 cm. The computational geometry of the heat pipe with macro inserts was prepared using the Solidworks software as shown in Figs. 2 and 3. The temperature and velocity contours obtained during the analysis using the ANSYS software are shown in Figs. 4 and 5.

Table 2. Properties of nano material.

Nano-particles and nanofluid sample	Thermal conductivity, W/(m K)	Specific heat, J/(kg K)	Density, g/m³	Reference
Al_2O_3	40	880	3700	[1,2]
ZnO	29	544	5600	[1,2]
CuO	77	540	6800	[1,2]
SiO_2	1.39	745	2220	[1,2]
TiO_2	11.2	650	3900	[1,2]
Al_2O_3 + ZnO + H_2O	0.80831	2958.44	1370.9	-

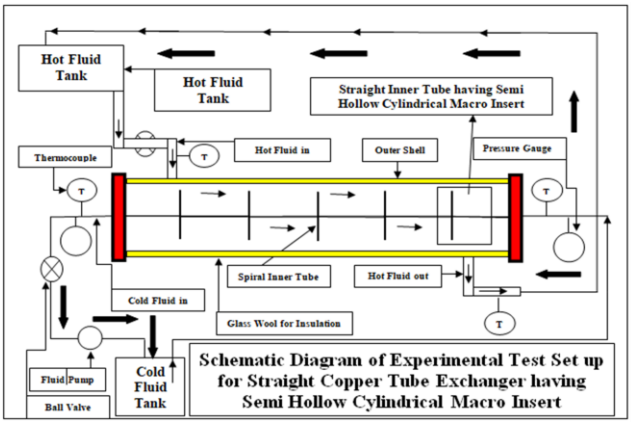

Fig. 1. Line diagram of experimental setup.

3. Grid independence procedure and testing result

Firstly, after completing all processes in the design modeller, the geometry is opened in the mesher. In the first step, a coarse mesh was generated, in subsequent steps the mesh was gradually refined. After the meshing was completed, the meshed geometry was solved in the solver. After the solution was converged, values of the essential parameters as required were obtained. The number of nodes for subsequent meshes, and the obtained corresponding values of the Nusselt number can be seen in Figs. 6 and 7.

Increasing the number of mesh nodes and repeating the computations was carried out until the solved values no longer varied with the mesh refinement. The process of grid independence investigations was terminated if the value of the crucial parameter with respect to that found for the previous mesh was less than one percent.

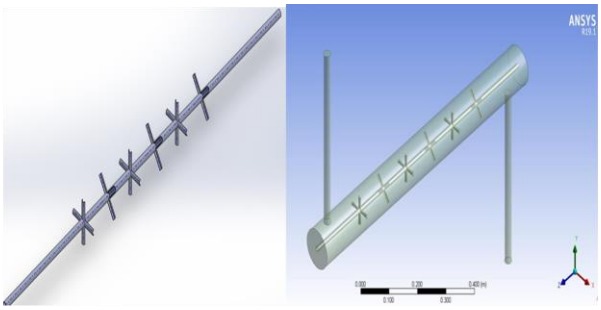

Fig. 2. Macro insert model.

Fig. 3. Computational geometric model.

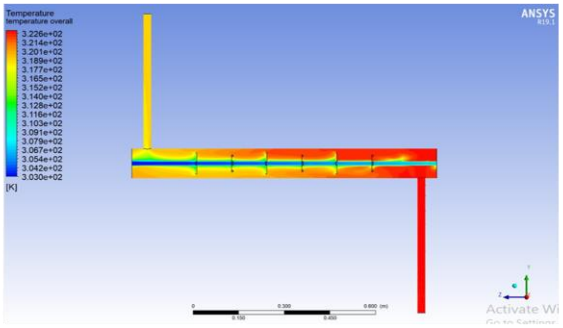

Fig. 4: Temperature distribution.

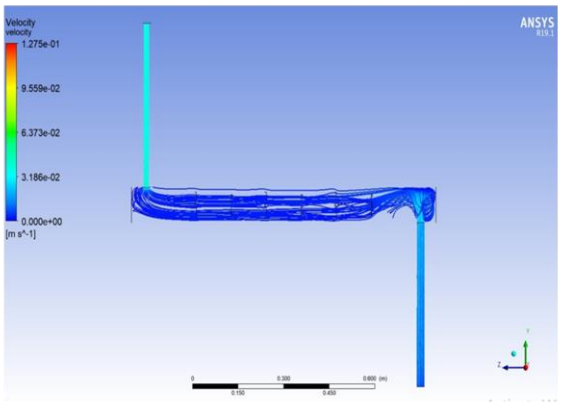

Fig. 5: Velocity contours.

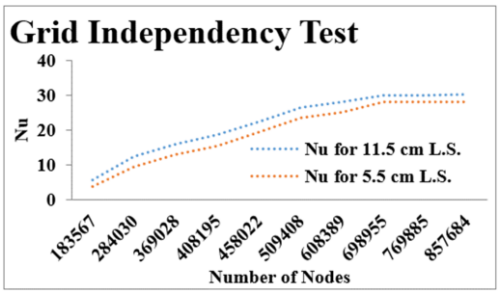

Fig. 6. Grid independence test of computational geometry.

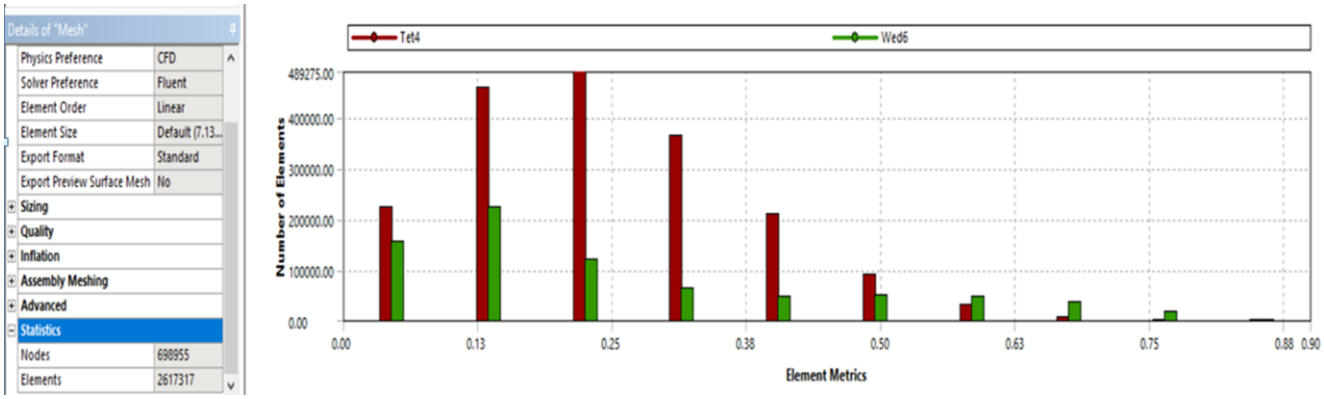

Fig. 7. Grid independence interface.

4. Data reduction

Experiments were carried out for different temperature fluids at diverse flow rates determined by the following equations

$$Q_{ds} = \frac{V}{t} \quad \text{where: } Q_{ds} = Area \cdot u, \tag{1}$$

$$m = \rho\, A\, u\,. \tag{2}$$

The heat transfer rate was obtained by the following equations:

$$Q_{hf} = m_{hf}\, C_{phf}(T_{in} - t_{out}) = Q_{cf} = m_{cf}\, C_{pcf}(T_{out} - t_{in}), \tag{3}$$

where T_{in} – outer GI shell tube inlet temperature, T_{out} – outer GI shell tube outlet temperature, t_{in} – spiral inner tube inlet temperature and t_{out} – spiral inner tube outlet temperature.

The heat transfer coefficient h and overall heat transfer coefficient U were calculated using the Log Mean Temperature Difference (LMTD) method and the equations used are as follows:

$$Q_r = h\, A\, \Delta T, \tag{4}$$

where:

$$\Delta T = \frac{(\Delta T_1 - \Delta T_2)}{\ln\left(\frac{\Delta T_1}{\Delta T_2}\right)},$$

$$\Delta T_1 = (T_{out} - T), \quad \Delta T_2 = (T - T_{out}),$$

$$U = h\, \frac{1}{\left(\frac{1}{h_i} + \frac{1}{h_o}\right)}. \tag{5}$$

Now, fluid properties for cold fluid are calculated by the following formulas:

$$\mathrm{Nu} = \frac{h\,D}{K_{cf}} = 0.023\mathrm{Re}^{0.8}\mathrm{Pr}^{0.4}, \quad \text{where: } Re = \frac{\rho u D}{\mu}, \tag{6}$$

$$f = \frac{\Delta P}{\left(\frac{L}{D}\right)\left(\frac{\rho V^2}{2}\right)}. \tag{7}$$

The performance parameters are further calculated for cold fluid flow:

$$\varepsilon = \frac{Q_{actual}}{Q_{max}}, \tag{8}$$

$$\mathrm{NTU} = \frac{U\, A_s}{(C_p)_{min}}, \tag{9}$$

where:

$$C = \left(mC_p\right)_{min}, \mathrm{NTU}_{\mathrm{counter}} = \frac{1}{c-1}\ln\left(\frac{\varepsilon - 1}{\varepsilon c - 1}\right), \tag{10}$$

$$\eta_{thpf} = \frac{\left(\frac{\mathrm{Nu}}{\mathrm{Nu}_{\mathrm{st}}}\right)}{\left(\frac{f^{0.33}}{f_{st}{}^{0.33}}\right)}, \tag{11}$$

$$\mathrm{Nu}_s = 0.023\mathrm{Re}^{0.8}\mathrm{Pr}^{0.4}, [8], \tag{12}$$

$$f_s = 0.316\mathrm{Re}^{-0.25}\,, [8]. \tag{13}$$

5. Results and discussion

In this research, fluid flow properties were investigated. The effects of nanofluid H_2O + ZnO + Al_2O_3 at 0.1% volume fraction inside a circular tube with macro inserts having LS of 11.5 cm and 5.5 cm are shown in Figs. 8–11 and 12.

Thermal behaviour of fluid was acknowledged for a range of Re number from 999 to 9 995 under counter flow conditions. Fluid flow peculiarities like the f factor and Nu number vary from 0.0992 to 0.0530 (simu. – simulated values), 0.00959 to 0.0529 (exp. – experimental values) and 11.21 to 30.33 (simu.), 10.81 to 29.75 (exp.) for 11.5 cm LS, whereas they change from 0.0998 to 0.0523 (simu.), 0.00932 to 0.0252 (exp.) and 9.86 to 23.65 (simu.), 9.49 to 23.04 (exp.) for 5.5 cm spacing. It has been clearly visible that the simulated results for the f factor show a decreasing trend and those of the Nu number show an increasing trend as the Re number and flow rate increase [14–15]. An enhancement of 3–6% in simulated values was acknowledged compared with experimental values for all profiles as shown in Figs. 8–11 and 12.

On the other hand, thermal performance peculiarities like f/fs and $\mathrm{Nu}/\mathrm{Nu}_s$ show an opposite trend compared with that of f factor and Nu number. Here, the f/f_s factor increases with a decreasing $\mathrm{Nu}/\mathrm{Nu}_s$ [14–15]. These values vary from 0.52 to 1.364 (simu.), 0.050 to 1.362 (exp.) and 0.132 to 0.051 (simu.), 0.133 to 0.421(exp.) for 11.5 cm LS, whereas they vary from 0.171 to 1.09 (simu.), 0.172 to 1.785 (exp.) and from 0.1325 to 0.0512 (simu.), 1.145 to 0.0326 (exp.) for 5.5 cm spacing. It is also

clearly visible that only Q shows an increasing trend, whereas ε, TPF and NTU show a decreasing trend as the Re number increases for 11.5 cm LS [14–15].

The thermal performance peculiarities are higher for 11.5 cm LS than for 5.5 cm spacing, where Q (*htr*) values vary from 171.55 to 269.40 (simu.), 170.59 to 268.40 (exp.) and ε varies from 0.26 to 0.171 (simu.), 0.128 to 0.126 (exp.), TPF obtained

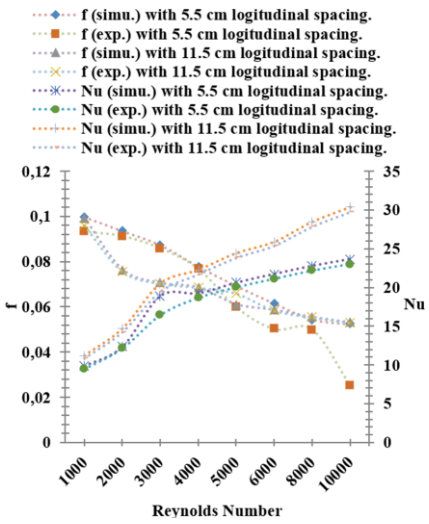

Fig. 8. Dependence of *f* and Nu on Re.

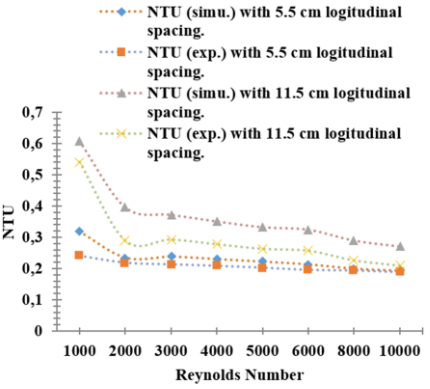

Fig. 9. Dependence of NTU on Re.

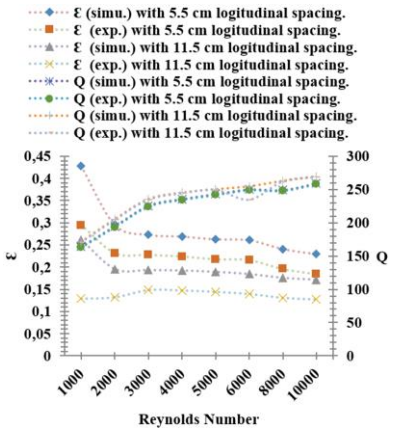

Fig. 10. Dependence of ε and Q (*htr*) on Re.

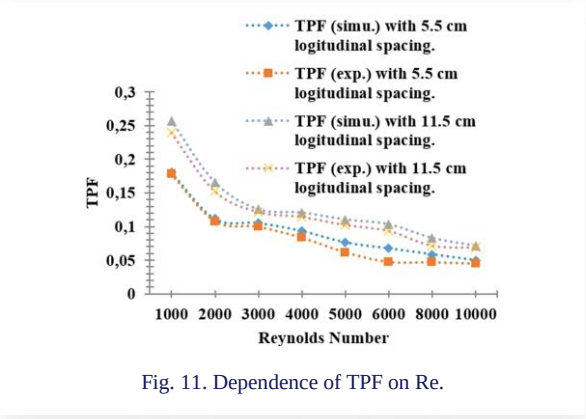

Fig. 11. Dependence of TPF on Re.

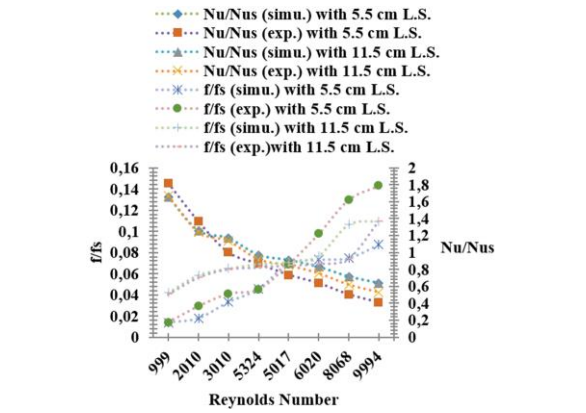

Fig. 12. Dependence of Nu/Nu_s and f/f_s on Re.

0.257 to 0.071 (simu.), 0.239 to 0.068 (exp.) and NTU 0.607 to 0.269 (simu.), 0.54 to 0.209 (exp.) for 11.5 cm spacing. TPF is an important heat exchanger parameter that has been identified to acknowledge the exchanger utilization aspect from Eq. (11). It is the ratio of a real value or a simulated value of the Nu number of the tube with insert to that of the smooth tube divided by the ratio of the f factor of the tube with insert to that of the smooth tube, expressed in a power of 0.33. The TPF values shown in Fig. 11 exhibit a decrease as the Re number rises when comparing smooth and insert-equipped tube performance, Fig.12. is utilized to indicate the performance improvement in the area. It is shown that smooth tubes perform inefficiently low at lower Re numbers and marginally well at higher Re numbers. The insert-equipped tubes exhibit much better results in both Reynolds number regions compared with smooth tubes. However, a decreasing trend of TPF values implies that the Nu ratio and f factor ratio are higher and lower in the low Re range, whereas the Nu ratio and f factor ratio are lower and higher in the high Re range between the smooth tube and insert-equipped tube, that is why TPF decreases with higher value of Re number. It has been discovered that 11.5 cm LS inserts work better than 5.5 cm LS.

6. Conclusions

Geometrical parameters, thermal conductivity and volume fraction play an important role in heat exchanger efficiency. This research focused on the thermal and fluid flow characteristics of

the proposed nanofluid. The effect of rectangular micro inserts was also acknowledged at 4 cm height and diversified longitudinal spacing, i.e. 5 cm and 11.5 cm. The present study was based on experimental and simulation investigations, leading to the following conclusions:

1. The obtained simulation results were validated with the experiment, and were found in a good agreement with experimental results with an error of 3 to 5%.
2. It was observed that semi-hollow cylindrical macro inserts produce more turbulence at 11.5 cm LS and 4 cm height with nanofluid Al_2O_3 + ZnO + H_2O when compared with other profiles. It happens because of the curved shape and extra exposed area of inserts.
3. The flow was maintained turbulent throughout the pipe with the micro inserts. The location and orientation of the micro inserts should be appropriate to get a constant production of turbulence.
4. The thermal performance rate at 11.5 cm LS increased by 20% when compared with 5.5 cm LS.
5. A 30% heat transfer enhancement was observed at 11.5 cm LS when compared with other configurations.
6. It is also concluded that nanofluid with a geometrical profile having macro-inserts at 11.5 cm longitudinal spacing shows better results as compared to other profiles at the optimum operating point, where the flow rate is 0.083 kg/s, Nu is 29.75, *f* factor is 0.052, *htr* is 268.40 J/s and ε is 0.126.

The present work has a wide scope of application in thermal engineering, power, aviation, space and automobile sectors, as these sectors use concentric tube heat exchangers in diverse applications. This work on nanofluids opens a new domain for research and various opportunities that lie in analysing different thermally feasible materials for enhancement of heat transfer. The effect of perforation in inserts will be analyzed in future for economical perspective and lowering material cost of concentric tube heat exchangers.

Acknowledgements

This research project is supported by Kumar Infratrade Pvt. Ltd. and infrastructure is provided by Shivalik College of Engineering, Dehradun.

References

[1] Chamsa-ard, W., Brundavanam, S., Fung, C., Fawcett, D., & Poinern, G. (2017). Nanofluid types their synthesis properties and incorporation in direct solar thermal collectors. A review. *Nano materials (MPDI)*, 7(6), 1–131. doi: 10.3390/nano7060131

[2] Qi, C., Luo, T., Liu, M., Fan, F., & Yan, Y. (2019). Experimental study on the flow and heat transfer characteristics of nanofluids in double-tube heat exchangers based on thermal efficiency assessment. *Energy Conversion and Management*, 197, 11187. doi: 10.1016/j.enconman.2019.111877

[3] Alimoradi, A., & Veysi, F. (2016). Prediction of heat transfer coefficient of shell and coiled tube heat exchanger. *International Journal of Thermal Science*, 107, 196–208. doi: 10.1016/j.ijthermalsci.2016.04.010

[4] Zhai, X., Qi, C., Pan, Y., Luo, Y., & Lian, L. (2019). Effect of screw pitches and rotation angles on flow and heat transfer characteristics of nanofluids in spiral tubes. *International Journal of Heat and Mass Transfer*, 130, 989–1003. doi: 10.1016/j.ijheatmasstransfer.2018.10.131

[5] Chandrasekar, M., Suresh, S., & Bose, A.C. (2010). Experimental Studies on heat transfer & friction factor characteristics of Al_2O_3/H_2O nanofluids in a circular pipe under laminar flow with wire coil insert. *Experimental Thermal and Fluid Science*, 34, 122–130. doi: 10.1016/j.expthermflusci.2009.10.001

[6] Ambreen, T., & Kim, M. (2018). Effect of variable particle sizes on hydrothermal characteristic of nanofluids in a micro channel. *International Journal of Heat and Mass Transfer*, 120, 490–498. doi: 10.1016/j.ijheatmasstransfer.2017.12.067

[7] Schuller, M., Show, Q., & Lalk, T. (2015). Experimental investigation of the specific heat of a nitrate – alumina nanofluid for solar thermal energy storage systems. *International Journal of Thermal Science*, 91, 142–145. doi: 10.1016/j.ijthermalsci.2015.01.012

[8] Kumar, N., Sonawane, S.S., & Sonawane, S.S. (2018). Experimental study of thermal conductivity, heat transfer and friction factor of Al_2O_3 based nanofluid. *International Communications in Heat and Mass Transfer*, 90, 1–10. doi: 10.1016/j.icheatmasstransfer.2017.10.001

[9] Kaushik, S., & Singh, S. (2019). Analysis on heat transmission and fluid flow attributes in solar air accumulator passage with diverse faux jaggedness silhouettes on absorber panel. *International Journal of Engineering and Advanced Technology*, 8, 32–41. doi: 10.35940/ijeat.E1011.0785S319

[10] Kaushik, S., Panwar, K., & Vashisth, S. (2022). Investigating the Thermionic Effect of Broken Perforated Curved Ribs on Solar Preheater through CFD Simulation. *Res Militaris*, 12(5). 1508-1524. https://resmilitaris.net/index.php/resmilitaris/article/view/2286/2139

[11] Abulkhair, H., Alsaiari, A.O., Ahmed, I, Almatrafi, E., Madhukeshwara, N., & Sreenivasa, B.R., (2023). Heat transfer and airflow friction in solar air heaters: A comprehensive computational and experimental investigation with wire-roughened absorber plate, Case Studies in Thermal Engineering, 48, 103148. doi: 10.1016/j.csite.2023.103148

[12] Uniyal, V., Kumar, J., S., Kaushik, S., & Kanojia, N. (2021). CFD Investigation of transfer of the heat and turbulent flow in circular copper tube with perforated conical rings of aluminium material. *Materials Today: Proceeding*, 46(15), 6719–6725. doi: 10.1016/j.matpr.2021.04.217

[13] Kaushik, S., Singh, S., Kanojia, N., Rawat, K., & Panwar, K. (2020). Comparative Study for Thermal and Fluid Flow Peculiarities in Cascading Spiral Inner Tube Heat Exchanger with or without Diverse Inserts over Spiral Tube. *IOP Conference Series: Materials Science and Engineering*, 802. doi: 10.1088/1757-899X/802/1/012009

[14] Kaushik, S., Singh, S., & Panwar, K. (2021). Comparative analysis of thermal and fluid flow behavior of diverse nanofluid using Al2O3, ZnO, CuO nanomaterials in concentric spiral tube heat exchanger. *Materials Today: Proceedings*, 46(15), 6625–6630. doi: 10.1016/j.matpr.2021.04.100

[15] Kaushik, S., Singh, S., & Panwar, K. (2022). Experimental Study of Fluid Flow Properties in Spiral Tube Heat Exchanger with Varying Insert Shape over Spiral Tube Profile. *Materials Today*. Proceeding Elsevier. 80(1), 78–84. doi: 10.1016/j.matpr.2022.10.117

[16] Kaushik, S., Singh, S., Kanojia, N., Naudiyal, R., Kshetri, R., Paul, A.R., Kumari, R., Kumar, A., & Kumar, S. (2021). Effect of introducing a varying number of fins over LED light bulb on

thermal behavior. *Materials Today: Proceeding*, 46(19), 9794–9799. doi: 10.1016/j.matpr.2020.10.876

[17] Kanojia, N., Kaushik, S., Singh, M., & Sha, M.K. (2021). A Comprehensive Review on Packed Bed Thermal Energy Storage System. In *Lecture Notes in Mechanical Engineering*, 1, 165–174. Springer Nature Singapore. doi: 10.1007/978-981-16-0942-8

[18] Yang, X., & Cai, Z., (2019). An analysis of a packed bed thermal energy storage system using sensible heat and phase change materials, International Journal of Heat and Mass Transfer, 144, 118651. doi: 10.1016/j.ijheatmasstransfer.2019.118651

[19] Kaushik, S., Panwar, K., & Karki, S.S. (2022). Comparative Thermal Analysis and Characteristic Optimization of Cram Bed Regenerator for Space Warmth Applications in Mountainous Areas. *Res Militaris* (resmilitaris.net), 12(5), 1525-1539. https://resmilitaris.net/index.php/resmilitaris/article/view/2287/2140

[20] Kanojia, N., Kaushik, S., Panwar, K., Kshetri, K., Uniyal, V., & Singh, M. (2021). Experimental investigation of optimum charging and discharging time on packed bed heat regenerator for space heating and solar drying application. *Materials Today: Proceedings*, 46(15), 6712–6718. doi: 10.1016/j.matpr.2021.04.210

[21] Elouali, A., Kousksou, T., Rhafiki, T., E., Hamdaoui, S., Mahdaoui, M., Allouhi, A., & Zeraouli, Y., (2019). Physical models for packed bed: Sensible heat storage systems, Journal of Energy Storage, 23, 69-78. doi: 10.1016/j.est.2019.03.004

[22] Panwar, K., & Kaushik, S. (2022). Investigation of Thermo-Mechanical Properties of Flue Gases Using CFD in Thermal Regenerator. *Res Militaris* (resmilitaris.net), 12(5), 1366-1376. https://resmilitaris.net/index.php/resmilitaris/article/view/2271/2124

[23] Sati, V., Kaushik, S., Kshetri, R., Panwar, K., & Pandey, R. (2020). Comparison of a Classical Cyclone Separator and Protruding Surface Cyclone Separator using CFD Software. *IOP Conference Series: Materials Science and Engineering*, 802, *2nd International Conference on Futuristic Trends in Materials and Manufacturing 2019*, 8-9th November 2019, Greater Noida, India. doi: 10.1088/ 1757-899X/802/1/012008

[24] Sati, V., Kaushik, S., Singh, S., Kshetri, R., & Pandey, R. (2019). Reduction of Losses in 90 Degree Pipe Bends by Varying Design Parameters using CFD Software, *International Journal of Engineering and Advanced Technology*, 8, 78–87. doi: 10.35940/ijeat.E1022.0785S319

[25] Kaushik, S., Sati, V., Kanojia, N., Mehra, K.S., Malkani, H., Pant, H., Gupta, H., Singh, A.P., Kumar, A., Paul, A.R., & Kumari, R. (2021). Bio-Diesel a Substitution for Conventional Diesel Fuel: A Comprehensive Review. In *Lecture Notes in Mechanical Engineering*, 1, 113–122. Springer Nature Singapore. doi: 10.1007/978-981-16-0942-8

[26] Kaushik, S., Pandey, R., & Singh, A. (2023). Industrial Automation System and its effect on the position of laborers and their consciousness. *Journal for ReAttach Therapy and Developmental Diversities*, 6(2s), 159–163. https://jrtdd.com/index.php/journal/article/view/276/212

[27] Kaushik, S., Singh, A., & Kumar, G. (2022). A Comprehensive Study on the Utilization of the Energy Using Mobile Solutions. *Res Militaris* (resmilitaris.net). 12(5), 1487–1497. https://resmilitaris.net/index.php/resmilitaris/article/view/2284/2137

[28] Kaushik, S., Ali, S., Kanojia, N., Uniyal, V., Verma, A.K., Panwar, S., Uniyal, S., Goswami, S., Kindo, S., Som, D., & Yadav, N.K. (2023). Experimental and CFD analysis of fluid flow in a rectangular strip-based microchannel with nanofluid. *Materials Today: Proceedings*. doi.: 10.1016/j.matpr.2023.05.647

[29] Kaushik, S., Verma, A., K., Singh, S., Kanojia, N., Panwar, S., Uniyal, S., Goswami, S., Kindo, S., Som, D., & Yadav, N.K. (2023). Comparative Analysis of Fluid Flow Attributes in Rectangular Shape Micro Channel having External Rectangular Inserts with Hybrid Al2O3+ZnO+H2O Nano Fluid and (H2O) Base Fluid. *EVERGREEN Joint Journal of Novel Carbon Resource Sciences & Green Asia Strategy*, 10(2), 851–862. doi: 10.5109/6792839

[30] Kaushik, S., Uniyal, V., Ali, S., Kanojia, N., Verma, A.K., Joshi, S., Makhloga, M., Pargai, P., S., Sharma, S.K., Kumar, R., & Pal, S. (2023). Comparative analysis of fluid flow in a mini channel with nanofluids and base fluid. *Materials Today: Proceedings*. doi: 10.1016/j.matpr.2023.05.363

[31] Kaushik, S., Uniyal, V., Verma, A.K., Jha, A.K., Joshi, S., Makhloga, M., Pargai, P., S., Sharma, S.K., Kumar, R., & Pal, S. (2023). Comparative Experimental and CFD Analysis of Fluid Flow Attributes in Mini Channel with Hybrid CuO+ZnO+H2O Nano Fluid and (H2O) Base Fluid. *EVERGREEN Joint Journal of Novel Carbon Resource Sciences & Green Asia Strategy*, 10(1), 182–195. doi: 10.5109/6781069

[32] Mehra, K.S., Kaushik, S., Pant, G., Kandwal, S., & Singh, A.K. (2021). Finite Element Modeling and Parametric Investigation of Friction Stir Welding (FSW). *Advances in Industrial Machines and Mechanisms, Lecture Notes in Mechanical Engineering*, 1, 251–259. doi: 10.1007/978-981-16-1769-0_23